BILINGUAL PUBLISHING GROUP

Journal of Environmental & Earth Sciences
https://journals.bilpubgroup.com/index.php/jees

ARTICLE

Exploring Variability in Sea Level at a Tide Gauge Station through Control Charts

H. Bâki İz

Independent Scholar, Boca Raton Florida, 33496, USA

ABSTRACT

Monitoring temporal changes in sea level is important in assessing coastal risk. Sea level anomalies at a tide gauge station, if kinematically conceived, include systematic variations such as trend, acceleration, periodic oscillations, and random disturbances. Among them, the non-stationary nature of the random sea level variations of known or unknown origin at coastal regions has been long recognized by the sea level community. This study proposes the analyses of subgroups of random residual statistics of a rigorously formulated kinematic model solution of tide gauge variations using X-bar and S control charts. The approach is demonstrated using Key West, Florida tide gauge records. The mean and standard errors of 5-year-long subgroups of the residuals revealed that sea level changes at this location have been progressively intensifying from 1913 to the present. Increasing oscillations in sea level at this locality may be attributed partly to the thermal expansion of seawater with increasing temperatures causing larger buoyancy-related sea level fluctuations as well as the intensification of atmospheric events including wind patterns and the impact of changes in inverted barometer effects that will alter coastal risk assessments for the future.

Keywords: Climate change; Sea level variance; X-bar; S control charts

1. Introduction

Monitoring sea level changes during the 20th and 21st centuries is important in assessing anthropogenic contributions to climate change mechanisms [1]. Recent sea level rise studies emphasize observing systematic changes, such as trends, accelerations, periodic oscillations, and unexplained random contributors to sea level changes of known or unknown origin.

*CORRESPONDING AUTHOR:
H. Bâki İz, Independent Scholar, Boca Raton Florida, 33496, USA; Email: h.baki.iz@gmail.com

ARTICLE INFO
Received: 23 September 2023 | Revised: 9 December 2023 | Accepted: 19 December 2023 | Published Online: 27 December 2023
DOI: https://doi.org/10.30564/jees.v6i1.5983

CITATION
İz, H.B., 2024. Exploring Variability in Sea Level at a Tide Gauge Station through Control Charts. Journal of Environmental & Earth Sciences. 6(1): 11–18. DOI: https://doi.org/10.30564/jees.v6i1.5983

Among them, systematic sea level changes are induced by wind stress, atmospheric pressure, precipitation, river discharge, currents, temperature and salinity of the water long periodic solar radiation variations and lunar tidal activities [2]. Sub-seasonal to decadal periodic movements of sea level, locally and regionally, are also induced by atmospheric pressure variations, sea surface winds, and ocean circulation patterns [3]. Linear and nonlinear systematic changes in sea level are represented by trend and acceleration/deceleration respectively using kinematic models.

Random sea level anomalies are due to the instrumental errors and transient roughness of the sea level over short or long timescales because of climatic changes. Irregular and episodic discharges from a nearby river, or seasonal variations due to the components of atmospheric pressure or temperature variations may have random components. Some of the sea level variability is attributed to the thermal expansion of seawater, which accelerates with increasing temperature and larger buoyancy-related sea level fluctuations [4]. Climate model simulations with increasing greenhouse gas emissions suggest that future sea level variability, such as the annual and interannual oscillations that alter local astronomical tidal cycles and contribute to coastal impacts, are expected to increase in many regions [4].

Recently, Woodworth et al. [5] stated that coastal sea level variability can be better understood than those in the deep ocean. Their study discussed the underlying forcing factors exhaustively. The systematic components of resulting coastal sea level variability can be modeled kinematically, which will be demonstrated as a byproduct of this study, such that the remaining unknown or unmodeled random variability in sea level can be scrutinized at tide gauge (TG) stations. Increasing oscillations in sea level are expected due to the thermal expansion of seawater with increasing temperatures causing larger buoyancy-related sea level fluctuations as well as the observed intensification of atmospheric events because of climate change [6] that will alter coastal risk assessments for the future.

The random appearance of the sea level changes has long been identified as having non-stationary properties [3]. The stationarity of random sea level variations can be understood formally as the statistical properties of a physical system that remain unchanged over time [7]. Two types of stationary series are identified: One having a *constant mean* and another, fluctuating about that mean with a *constant variance* [8]. A study by Iz and Ng [9], already demonstrated by examining globally distributed 1862 stations' tide gauge data from the Permanent Service for Mean Sea Level (PSMSL) that random excursions in sea levels are preponderantly *non-stationary in variance*. This study conjures further and demonstrates that there is more to be learned from the time progression of *non-stationary variances* in sea level anomalies for climate change related risk assessments at coastal regions.

In the following sections, the Key West TG station record is used to examine the random properties of the sea level fluctuations at this locality as an example. Systematic and random sea level variations observed at this station are represented by a rigorous kinematic model. An Ordinary Least Squares (OLS) solution to the kinematic model is then carried out and the solution residuals are analyzed using their subgroups' statistics inspired by X-bar and S control charts. The reliability of the finding, an increase in the variance of the random changes in sea level at this TG station from 1913 to the present, is quantified by bootstrapping the residuals and analyzing alternative random realization of residual subgroups' stationary/non-stationary properties.

2. An extended kinematic model of sea level variations

The following extended kinematic model represents observed sea level height anomalies at a TG station. It consists of a trend, a uniform acceleration, and periodic sea level variations to represent observed sea level anomalies h_t^{obs} at an epoch t with random disturbances ε_t,

$$h_t^{obs} = h_0 + v_0(t - t_0) + \frac{a}{2}(t - t_0)^2 + \\ + \sum_{h=1}^{17} \left\{ \alpha_h \sin\left[\frac{2\pi}{P_h}(t - t_0)\right] + \gamma_h \cos\left[\frac{2\pi}{P_h}(t - t_0)\right] \right\} + \varepsilon_t \quad (1)$$

where, the reference datum h_0 is defined in the middle of the record at an epoch t_0. The trend is the initial velocity v_0 at t_0 when $a \neq 0$, and a is the constant rate of change in the sea level velocity (i.e., the uniform acceleration). P_h are the periods of systematic sea level oscillations. Their amplitudes can be constructed using α_h *and* γ_h sin and cosine components respectively.

What is markedly different in this model as compared to the previous studies of a similar nature① is the inclusion of various prospective low frequency sea level variations at a TG station explicitly in a top-down approach. The origins of these oscillations in sea level were conjured by Munk et al. [10] and Keeling and Whorf [11]. Under their scenarios, interactions of the ocean, meteorological forcing, and sea surface temperature materialize as natural broad band sea level variations. They modulate astronomical forcings, such as lunar node tide systematically or as random beatings resulting in sub and super harmonics of known periods (**Table 1**). Similarly, the variations in total solar radiation with a period of P = 11.1 years, yield subharmonics with periods: 2 × P = 22.2 years and longer. An earlier wavelet analysis by Yndestad [12] also identified several lunar node subs and super harmonics in Arctic Sea level, temperature, ice extent and winter index time series data, including the signature of nodal harmonics in pole position time series (**Table 1** in Yndestad [13]), and a strong cross correlation with Chandler wobble.

Although the observed amplitudes of such oscillation are small, they can bias sea level trends and acceleration estimates. Their unmodeled effects confound short TG and Satellite Altimetry, SA, time series thereby hindering the search for a global GMSL acceleration caused by anthropogenic global warming. İz [14] demonstrated that once these effects are modeled and the corresponding model parameters are estimated, spectral analyses of the TG residuals reveal additional statistically significant sea level variations at the decadal scale due to the ocean surface wind forcings and periodic changes in atmospheric pressure along the coastal lines of some of the TG stations [15].

All the above-mentioned effects are therefore incorporated into the kinematic model. The periodicities consist of a mix of seventeen sub and super harmonics attributed to the compounding of the nodal tides, solar radiation, and annual and sub annual variations with natural sea level variations (**Table 1**). In total, the extended kinematic model includes 37 unknown parameters.

As far as the statistical properties of the model are concerned, the disturbances denoted by ε_t may be autocorrelated of first order, AR(1). First order autocorrelations AR(1) exist with varying magnitudes in globally distributed tide gauge stations once the low frequency sea level variations are modeled. The autocorrelations are always positive and can be as large as ρ = 0.4 or more. Such AR(1) disturbances can be represented as follows,

Table 1. Compounded Luni-Solar and other periodicities all in years.

Nodal subharmonics	Nodal superharmonics	Nodal superharmonics	Solar	Chandler	Annual subannuals
74.5	18.6	3.7	11.1	429.5/365.4 = 1.2	1.00
55.8	9.3	3.1	22.2		0.50
37.2	6.2	2.6	0.25		
	4.7	2.3			

① With the exception of the earlier studies by this investigator.

$$\varepsilon_t = \rho\varepsilon_{t-1} + u_t \tag{2}$$

In this expression, $-1 \le \rho \le 1$ is the unknown autocorrelation coefficient of the AR(1) process. Furthermore, the stochastic processes for the random noise u_t and ε_t, have the following assumed distributional properties,

$$E(u_t) = 0,\ E\left(u_t^2\right) = \sigma_u^2,\ E(u_t u_{t-1}) = 0 \tag{3}$$

where σ_u^2 is the variance of u_t. The square root of its estimate is denoted by, $\hat{\sigma}_u$ or stated simply as the standard error, SE. The error of omission of a positive AR(1) correlation reduces the effective length of the total series statistically in proportion to the magnitude of ρ, and leads to a Type I error in testing null-hypotheses when assessing the solution parameters. The above expression together with Equation (2) gives,

$$E(\varepsilon_t) = 0,\ E(\varepsilon_t^2) = \sigma_\varepsilon^2 = \frac{\sigma_u^2}{1-\rho^2} \tag{4}$$

If the observation equation represented by Equation (1) at an epoch t-1 is multiplied by ρ and subtracted from the following observation equation at t, the effect of AR(1) is removed,

$$\begin{aligned} h_t - \rho h_{t-1} = {} & \left[h_{t_0} - \rho h_{t_0-1}\right] + v_0[(t-t_0) + \rho(t_{t-1}-t_0)] \\ & + \frac{a}{2}\left[(t-t_0)^2 + \rho(t_{t-1}-t_0)^2\right] \\ & + \sum_{k=1}^{n}\left(\alpha_h \sin\left[\frac{2\pi}{P_k}(t-t_0)\right]\right. \\ & \left. - \rho\alpha_k \sin\left[\frac{2\pi}{P_k}(t_{t-1}-t_0)\right]\right) \\ & + \sum_{k=1}^{n}\left(\gamma_k \cos\left[\frac{2\pi}{P_k}(t-t_0)\right]\right. \\ & \left. - \rho\gamma_k \cos\left[\frac{2\pi}{P_k}(t_{t-1}-t_0)\right]\right) + u_t \end{aligned} \tag{5}$$

Because the random errors in this representation are identically and independently distributed, *i.i.d.*, with zero expected value, i.e., $u_t \sim (0, \sigma_u^2)$,the observation equations based on Equation (5) can be solved using the OLS method. In the following section, OLS is used to generate the residuals needed for the graphical analyses of random excursions in sea level at Key West, Florida TG station.

3. Tide gauge records

Key West, Florida, monthly TG time series data displayed in **Figure 1** are used for the OLS solution and the graphical analyses of the residuals. The record is referenced to the Revised Local Reference, RLR, defined by the Permanent Mean Sea Level, PSMSL. No corrections including post glacial rebound, nor inverted barometric effects were applied to the data. The records were downloaded from the PSMSL repository in November 2020 [16].

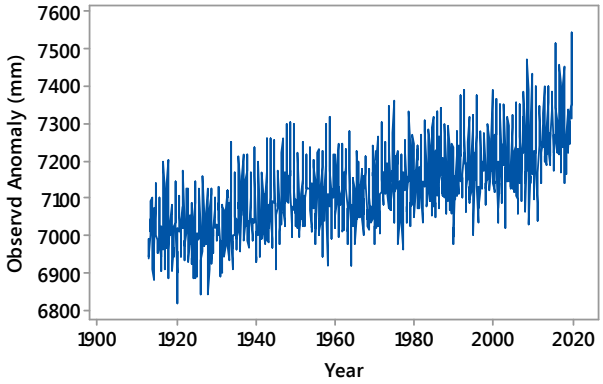

Figure 1. Monthly averaged sea level height anomalies at Key West, Florida, TG station.

4. Ordinary least squares solution

The observation equation given by Equation (5) is a function of the unknown AR(1) correlation coefficient ρ on the left-hand side. If several OLS solutions are carried out for the values within the interval $[-1 \le \rho \le 1]$, the solution with the smallest SE is adopted as the optimal value for the model based on Equation (5). This process is known as the Hildreth-Lu procedure [17]. All the statistically significant parameters for the Key West Florida TG station, i.e., those with p-values②, $p < 0.05$, were estimated using this approach.

The solution statistics tabulated in **Tables 2 and 3** indicate that the model explains more than 72% of the sea level variations together with well-defined

② *p-value* is the probability of obtaining a test statistic result at least as extreme or as close to the one that was observed, if the null hypothesis is true (Goodman, 1999). Smaller *p-values* for the model parameters in this study provide statistical evidence (*independent of the significance level*) that the magnitudes of estimates cannot be attributed to chance alone.

Table 2. OLS solution statistics. Trend and uniform acceleration estimates are statistically significant at $\alpha = 0.05$.

Time span year	Initial velocity mm/year	Uniform acceleration mm/year^2	SE mm.	Adj. R^2 %	DW	ρ
1913–2020	2.45 ± 0.06	0.018 ± 0.005	41.2	71.8	1.9	0.4

Table 3. Statistically significant amplitudes of periodicities and their SEs. Units are in mm.

Period (year)	75	37	37	12.4	11	6	Annual	Semi-annual
Amplitude	11.78	18.05	18.05	6.77	6.49	6.95	81.28	39.23
SE	±2.87	±2.89	±2.79	±2.76	±2.75	±2.70	±2.38	±1.87

sea level trends and uniform acceleration estimates. The Durbin-Watson statistic, DW = 1.9, is close to its expected value of 2, which indicates the solution residuals are free from unmodeled systematic effects.

The statistically significant low frequency sea level variations experienced at the TG station shown in **Table 3** have amplitudes large enough to bias the trend and acceleration estimates and their statistics. More importantly, they confound the randomness of the residuals if they are not incorporated into the model.

Figures 2 and 3 reveal that the residuals are unambiguously free from any unmodeled systematic sea level variations. This outcome is also a testament to the effectiveness of the top-down modeled low frequency sea level changes. Because the model removes all the systematic variations from the sea level anomalies, the remaining unexplained sea level variations at this TG station are the random effects whose statistical properties will be studied in the following section.

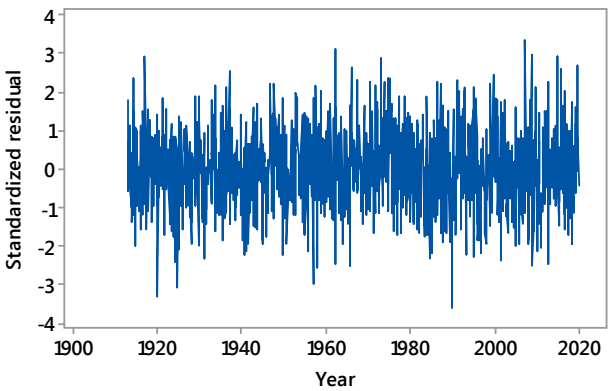

Figure 2. Standardized residuals (residuals divided by their standard errors).

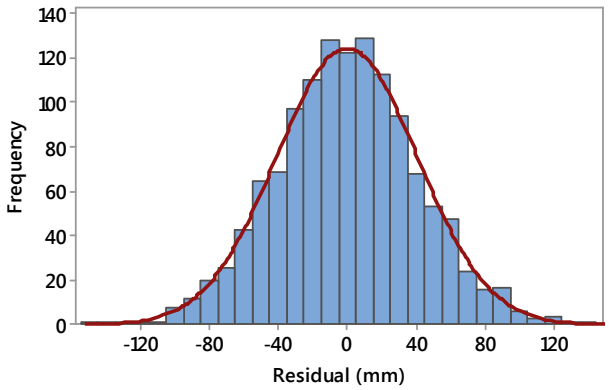

Figure 3. The histogram of the standardized residuals exhibits a normal-like distribution.

5. The analyses of the residuals using $\bar{x}$ and *s* control charts

In statistical quality control, X-bar and S control charts (also known as Shewhart charts [18]) are used to monitor variation in a business or industrial process during which samples are collected at regular intervals and analyzed [18]. In this study, inspired by these charts, subgroups of residuals will be created and the time evolution of their means and standard errors will be investigated using what is labelled in this study as X-bar and S control charts. As previously stated, part of the displayed sea level variability by these charts' statistics can be attributed to the thermal expansion of seawater, which is expected to increase with rising sea surface temperature in many regions as demonstrated by simulation studies [18].

A prerequisite for the analyses of the residual charts would be their randomness, i.e., Normal-like distribution of the standardized residuals shown in

Figure 2, and their statistical independence. The histogram with a Normal distribution fitting is shown in **Figure 3** and the DW test result confirms that the conditions for randomness are effectively fulfilled. The correlogram generated with 5-year lags reveals that there are no statistically significant leftover autocorrelations in the residual series (**Figure 4**).

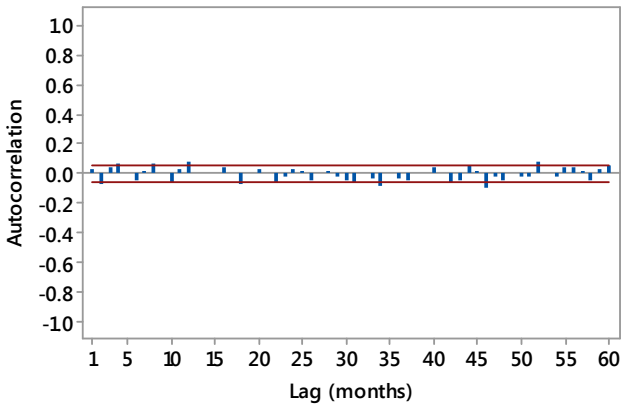

Figure 4. Correlogram of the residuals with 5% significance intervals based on 5-year lags.

At this point, X-bar and S residual charts can be constructed. **Figure 5** is the X-bar residual chart generated by the averages of 5-year subgroups standardized residuals. The time progression of the 5-year subgroup residual averages varies randomly about the zero mean of the entire standardized residuals series and reveals that the residuals are stationary in mean. But S residual chart exhibits a contiguously increasing variance in the sea level, i.e., residuals are non-stationary in variance (**Figure 6**). A simple linear regression, using the standard errors of the subgroup means as dependent variables, shows that there is a statistically significant ($\alpha = 0.05$) rate of increase of 0.009 ± 0.003 rad/year in sea level variance since 1913. For the moment, assessing the physical significance of the estimated rate increase would be challenging since this is an underresearched topic in sea level studies, which requires similar assessments at other globally distributed TG stations for clarity.

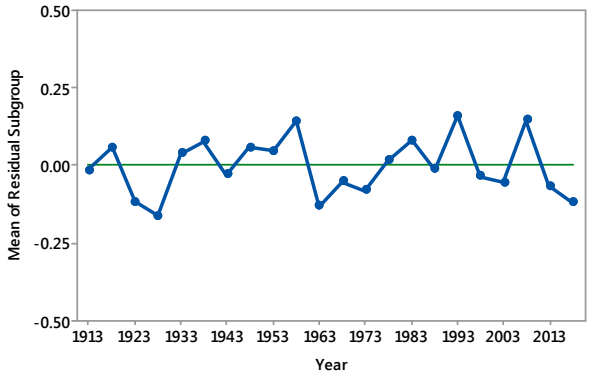

Figure 5. X-bar residual chart constructed using means of 5-year long subgroup residuals.

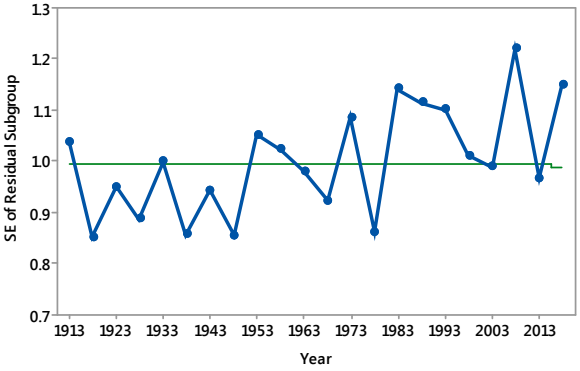

Figure 6. The S residual chart was constructed using the standard errors of 5-year long subgroups of residuals.

Meanwhile, although the trend of the S residual chart is statistically significant and visually noticeable on the graph, it is still questionable if the intensification is due to chance only, because the regression explains only Adj $R^2 = 28\%$ of the variation. To verify, one hundred monthly residual series were generated by randomly shuffling the original standardized residuals. The s residual charts were then created for each shuffled residual series and the trends of the s residual charts were estimated (**Figure 7**). Out of one hundred bootstrapped subgrouped S residual charts, only the trend of one series' S residual chart (shown in **Figure 7** with a red diamond shape) exceeded the trend of the original (shown as a red circular dot) indicating that the odds for getting the intensification of the residuals' variances of this magnitude by chance alone is about 1 out of 100.

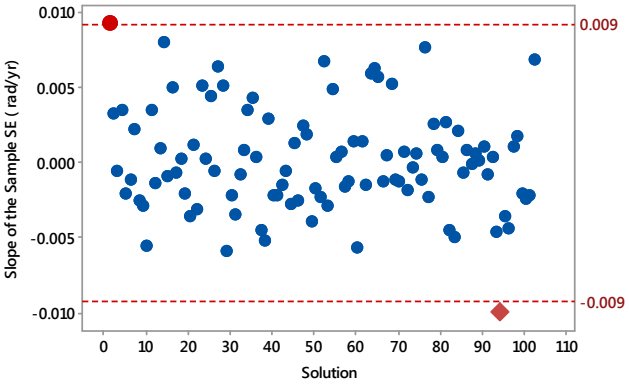

Figure 7. The S residual chart trends (rad/year) are estimated from the S residual charts of 100 randomly shuffled standardized monthly residual series. Red dot is the trend of the original series' residuals' S chart. Only one trend out of 100 bootstrapped series trends (shown with a red diamond shape) has a magnitude larger than the original trend of the *s* residual chart.

6. Conclusions

This study demonstrated the use of S residual charts to investigate random properties of sea level variations at Key West TG station. The residuals of an OLS solution to a rigorous kinematic model representing sea level anomalies revealed that random sea level fluctuations at this station are stationary, however, the variances of the random sea level changes have been steadily increasing since 1913 up to the present. Evidently, there is more to be learned about the nature of random sea level variations at globally distributed TG stations using graphical analyses of their stationary/non-stationary properties. The origin and potential ramifications of the increasing variance in sea level rise for coastal risk assessments will require further investigations.

Conflict of Interest

I declare no conflict of interest.

Funding

This research received no external funding.

Acknowledgement

I express my gratitude to the anonymous referees for dedicating their time and providing valuable comments.

References

[1] Climate Change 2001: The Scientific Basis [Internet]. IPCC [cited 2002 Sep 24]. Available from: https://www.ipcc.ch/report/ar3/wg1/

[2] Lambeck, K., 1980. Earth's variable rotation: Geophysical causes and consequences. Cambridge University Press: Cambridge. pp. 449.

[3] Pugh, D.T., 1987. Tides, surges and mean sea level. John Wiley & Sons Ltd.: Hoboken. pp. 300–330.

[4] Widlansky, M.J., Long, X., Schloesser, F., 2020. Increase in sea level variability with ocean warming associated with the nonlinear thermal expansion of seawater. Communications Earth & Environment. 1(1), 9.
DOI: https://doi.org/10.1038/s43247-020-0008-8

[5] Woodworth, P.L., Melet, A., Marcos, M., et al., 2019. Forcing factors affecting sea level changes at the coast. Surveys in Geophysics. 40(6), 1351–1397.
DOI: https://doi.org/10.1007/s10712-019-09531-1

[6] Bhatia, K.T., Vecchi, G.A., Knutson, T.R., et al., 2019. Recent increases in tropical cyclone intensification rates. Nature Communications. 10(1), 635.
DOI: https://doi.org/10.1038/s41467-019-08471-z

[7] Emery, W.J., Emery, W.J., 2001. Data analysis methods in physical oceanography, second and revised edition. Elsevier: Amsterdam. pp. 373–374.

[8] Kendall, M., 1973. Time-series, second edition. Charles Griffin and Company Ltd.: London. pp. 70–85.

[9] İz, H.B., Ng, H.M., 2005. Are global tide gauge data stationary in variance? Marine Geodesy. 28(3), 209–217.
DOI: https://doi.org/10.1080/01490410500204546

[10] Munk, W., Dzieciuch, M., Jayne, S., 2002. Millennial climate variability: Is there a tidal connection? Journal of Climate. 15(4), 370–385.
DOI: https://doi.org/10.1175/1520-0442(2002)

015<0370:MCVITA>2.0.CO;2

[11] Keeling, C.D., Whorf, T.P., 1997. Possible forcing of global temperature by the oceanic tides. Proceedings of the National Academy of Sciences. 94(16), 8321–8328.
DOI: https://doi.org/10.1073/pnas.94.16.8321

[12] Yndestad, H., 2006. The influence of the lunar nodal cycle on Arctic climate. ICES Journal of Marine Science. 63(3), 401–420.
DOI: https://doi.org/10.1016/j.icesjms.2005.07.015

[13] Yndestad, H., Turrell, W.R., Ozhigin, V., 2008. Lunar nodal tide effects on variability of sea level, temperature, and salinity in the Faroe-Shetland Channel and the Barents Sea. Deep Sea Research Part I: Oceanographic Research Papers. 55(10), 1201–1217.
DOI: https://doi.org/10.1016/j.dsr.2008.06.003

[14] Iz, H.B., 2006. How do unmodeled systematic mean sea level variations affect long-term sea level trend estimates from tide gauge data? Journal of Geodesy. 80, 40–46.
DOI: https://doi.org/10.1007/s00190-006-0028-x

[15] Iz, H.B., 2018. The effect of regional sea level atmospheric pressure on sea level variations at globally distributed tide gauge stations with long records. Journal of Geodetic Science. 8(1), 55–71.
DOI: https://doi.org/10.1515/jogs-2018-0007

[16] Tide Gauge Data [Internet]. Permanent Service for Mean Sea Level (PSMSL). Available from: http://www.psmsl.org/data/obtaining/

[17] Hildreth, G., Lu, T., 1960. Demand relations with autocorrelated disturbances. Michigan State University Agricultural Experiment Station: East Lansing.

[18] Shewhart X-bar and S Control Charts [Internet]. National Institute of Standards and Technology. Available from: https://www.itl.nist.gov/div898/handbook/pmc/section3/pmc321.htm